GEORGIA INSTITUTE OF TECHNOLOGY — OFFICE OF CONTRACT ADMINISTRATION

PROJECT ADMINISTRATION DATA SHEET

[x] ORIGINAL [ ] REVISION NO. _____

Project No. G-35-641 (G-35-329 c/s) DATE 2/16/82

Project Director: Dr. D. D. Davis School/~~Lab~~ Geo. Sci.

Sponsor: National Science Foundation

Type Agreement: Grant No. ATM-8113237

Award Period: From 1/15/82 To ~~12/31/83~~ 6-30-84 (Performance) 3/31/84 (Reports)

Sponsor Amount: $168,800 Contracted through:

Cost Sharing: $ 61,191 GTRI/~~GTRC~~

Title: Spectroscopy, Photochemistry and Kinetics

ADMINISTRATIVE DATA OCA Contact Linda H. Bowman x4820

1) Sponsor Technical Contact:

Richard A. Carrigan
National Science Foundation
Washington, DC 20550

(202) 357-9657

2) Sponsor Admin/Contractual Matters:

Mary Frances O'Connell
National Science Foundation
Washington, DC 20550

(202) 357-9602

Defense Priority Rating: none Security Classification: none

RESTRICTIONS

See Attached NSF Supplemental Information Sheet for Additional Requirements.

Travel: Foreign travel must have prior approval — Contact OCA in each case. Domestic travel requires sponsor approval where total will exceed greater of $500 or 125% of approved proposal budget category.

Equipment: Title vests with GIT

COMMENTS:

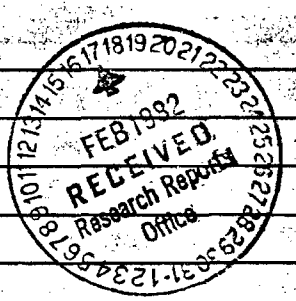

COPIES TO:

Administrative Coordinator	Research Security Services	EES Public Relations (2)
Research Property Management	~~Reports Coordinator (OCA)~~	Computer Input
Accounting	Legal Services (OCA)	Project File
Procurement/EES Supply Services	Library	Other

FORM OCA 4:78

GEORGIA INSTITUTE OF TECHNOLOGY OFFICE OF CONTRACT ADMINISTRATION

SPONSORED PROJECT TERMINATION/CLOSEOUT SHEET

Date 2/18/85

Project No. G-35-641 (C/S G-35-329) School/Lab ~~XXXXX~~ Geo Sci.

Includes Subproject No.(s) N/A

Project Director(s) Dr. D. D. Davis GTRI / ~~GXX~~

Sponsor National Science Foundation

Title Spectroscopy, Photochemistry and Kinetics

Effective Completion Date: 6/30/84 (Performance) 9/30/84 (Reports)

Grant/Contract Closeout Actions Remaining:

- [ ] None
- [X] Final Invoice or Final Fiscal Report
- [ ] Closing Documents
- [X] Final Report of Inventions
- [X] Govt. Property Inventory & Related Certificate
- [ ] Classified Material Certificate
- [ ] Other

Continues Project No. Continued by Project No.

COPIES TO:

Project Director
Research Administrative Network
Research Property Management
Accounting
Procurement/EES Supply Services
Research Security Services
~~Reports Coordinator (OCA)~~
Legal Services
Library
GTRI
Research Communications (2)
Project File
Other M. Heyser; A. Jones

Form OCA 60:1028

NATIONAL SCIENCE FOUNDATION
Washington, D.C. 20550

FINAL PROJECT REPORT
NSF FORM 98A

PLEASE READ INSTRUCTIONS ON REVERSE BEFORE COMPLETING

PART I–PROJECT IDENTIFICATION INFORMATION

1. Institution and Address	2. NSF Program	3. NSF Award Number
Georgia Institute of Technology School of Geophysical Sciences Atlanta, GA 30332	Atmospheric Sciences	ATM-8113237
	4. Award Period From 1/15/82 To 6/30/84	5. Cumulative Award Amount $168,825.00

6. Project Title
Spectroscopy, Photochemistry, and Kinetics of Several Iodine Compounds of Atmospheric Interest

PART II–SUMMARY OF COMPLETED PROJECT *(FOR PUBLIC USE)*

A laser flash photolysis apparatus has been used to measure absolute photoabsorption cross sections for the species IO and HOI, as well as rate coefficients for four gas phase reactions involving these molecules. The IO absorption spectrum is consistent with another published result (Cox and Coker, 1983), except in regard to the (0,0) band which was not observed in the present study. The cross section of the (4,0) band was found here to be $3.1 \pm 0.6 \times 10^{-17} cm^2$. The spectrum of HOI was found to resemble that of HOCl, however the peak cross section, $\sigma = 4 \times 10^{-17} cm^2$, is roughly 20 times the HOCl value and peaks at a wavelength of $\sim$ 340 nm. The following rate coefficients were obtained here: $k_1(I+O_3) = 1.2 \pm 0.2 \times 10^{-10}$, $k_3(IO+IO) = 6.6 \pm 1.1 \times 10^{-11}$, $k_4(O+I_2) = 1.44 \pm 0.24 \times 10^{-10}$, $k_{12}(OH+I_2 \rightarrow x) = 1.1 \pm 0.6 \times 10^{-10}$ (all in $cm^3 \cdot molec^{-1} \cdot sec^{-1}$) and k_{13} ($x \rightarrow HOI+I$) $\sim 2 \times 10^{-3} s^{-1}$. The value for k_3 differs substantially from other measurements (Cox and Coker, 1983; Jenkin and Cox, 1984) while the k_1 and k_4 are substantially in good agreement with previous investigations. The value of k_{12} and k_{13} are the first to be reported.

PART III–TECHNICAL INFORMATION *(FOR PROGRAM MANAGEMENT USES)*

1. ITEM *(Check appropriate blocks)*	NONE	ATTACHED	PREVIOUSLY FURNISHED	TO BE FURNISHED SEPARATELY TO PROGRAM	
				Check (√)	Approx. Date
a. Abstracts of Theses	√				
b. Publication Citations				√	July 1985
c. Data on Scientific Collaborators		√			
d. Information on Inventions	√				
e. Technical Description of Project and Results		√			
f. Other *(specify)*					

2. Principal Investigator/Project Director Name *(Typed)*	Signature	4. Date
Douglas Davis		2/6/85

NSF Form 98A (3-83) Supersedes All Previous Editions

Form Approved OMB No. 3145-0058

PART III.

b. Publications:

(1) Gas Kinetic Rate Coefficients for the Iodine Containing Rxs: $I + O_3$, $O + I_2$, and IO + IO, As Measured by the Method of Laser Flash Photolysis/Laser Absorption Spectroscopy. Intern'l. J. Chemical Kinetics.

(2) An Absorption Spectrum with Absolute Cross Sections for the IO Radical. J. Physical Chemistry.

(3) A Study of the Gas Phase Formation of HOI: A Tentative UV Absorption Spectrum. J. Physical Chem.

c. Scientific Collaborators:

Dr. John Bradshaw, Research Scientist II
Dr. Anthony Hynes, Postdoctoral Fellow
Dr. Robert Stickel, Postdoctoral Fellow

SPECTROSCOPY, PHOTOCHEMISTRY, AND KINETICS OF SEVERAL IODINE COMPOUNDS OF ATMOSPHERIC INTEREST

F I N A L R E P O R T

Submitted to:

NATIONAL SCIENCE FOUNDATION
1800 "G" Street N.W.
Washington, D.C. 20550.

Submitted by: Douglas D. Davis, Principal Investigator

Georgia Institute of Technology
School of Geophysical Sciences
Atlanta, Georgia, 30332.

I. INTRODUCTION

In recent years several authors (Chameides and Davis, 1980; Zafariou, 1975; Moyers and Duce, 1972) have suggested that iodine containing compounds may be important in tropospheric chemistry. For example, Chameides and Davis have suggested that the catalytic destruction of ozone by iodine may play a significant role in the N_xO_y and H_xO_y cycles. However, an accurate estimate of the importance of atmospheric iodine has been hampered by a lack of kinetic and photochemical information. The present report describes an experimental investigation undertaken to remove some of the major uncertainties identified by Chameides and Davis. The objectives of this study were (1) a quantitative investigation of the photoabsorption spectra of key iodine species such as IO, and HOI, (2) an investigation of the products of IO and HOI photolysis and (3) the direct measurements of the rate coefficients for several of the more important reactions involved in the production and destruction of the above iodine species. In spite of a major set-back due to vendor misrepresentation of the capabilities of a critically needed continuum light source (originally proposed for the photoabsorption measurements) most of these objectives have been attained.

As described in greater detail below, we have measured the photoabsorption spectrum of IO throughout the 417 - 470 nm region. In addition, we present here the first measurements of the absorption cross section for the species HOI. While the identity of the absorbing species has not been established beyond question, we present evidence which strongly confirms our identification. Finally, we include measured values of the rate coefficients for the reactions

$$I + O_3 \rightarrow IO + O_2$$

$$O + I_2 \rightarrow IO + I$$

$$IO + IO \overset{M}{\rightleftharpoons} I_2O_2$$

and $OH + I_2 \rightarrow HOI + I$

and we show results which suggest that this last reaction may proceed by a two step process. During the course of this work results on several of the proposed areas of investigation were published by Cox and Coker, 1983 and Jenkin and Cox, 1984. In general, these two independent investigations are in substantial agreement. However, there are some important disagreements which will be further discussed in the main text.

II. EXPERIMENTAL

The species of interest (IO, HOI) were produced by reaction sequences initiated by laser flash photolysis as described in a subsequent section of this report. Summaries of the three production mechanisms investigated in this work are included below.

Initially, IO was produced by the photolysis of I_2 at 532 nm in the presence of ozone, e.g.

$$I_2 + h\nu(\lambda=532\ nm) \rightarrow I + I\ (\Delta t \stackrel{\sim}{=} 10\ ns)$$

$$1)\quad I + O_3 \rightarrow IO + O_2$$

A complete kinetic model of this system must also include the competing I atom reaction:

$$2)\quad I + I \xrightarrow{M} I_2$$

and the principle IO loss channel,

$$3)\quad IO + IO \xrightarrow{M} I_2O_2$$

Immediately following the photolysis flash, typical concentrations are: $[I] \stackrel{\sim}{=} 2 \times 10^{14}$ and $[O_3] \stackrel{\sim}{=} 5 \times 10^{15}$ (molec$\cdot$cm^{-3}). Thus IO forms with a psuedo first-order time constant of about 200μs. However, when the IO concentration reaches the mid-10^{13} range, loss via reaction (3) becomes dominant. The resulting IO population curve is shown in figure 1. It is evident from this plot that the peak IO density is only about one-fourth of the initial I atom concentration. This result gives rise to two problems. Firstly, the IO concentration is strongly dependent on the rate coefficient used to model reaction (3). Any error in this rate leads to a corresponding error in the measured absorption cross-section. Secondly, while it is necessary to produce a

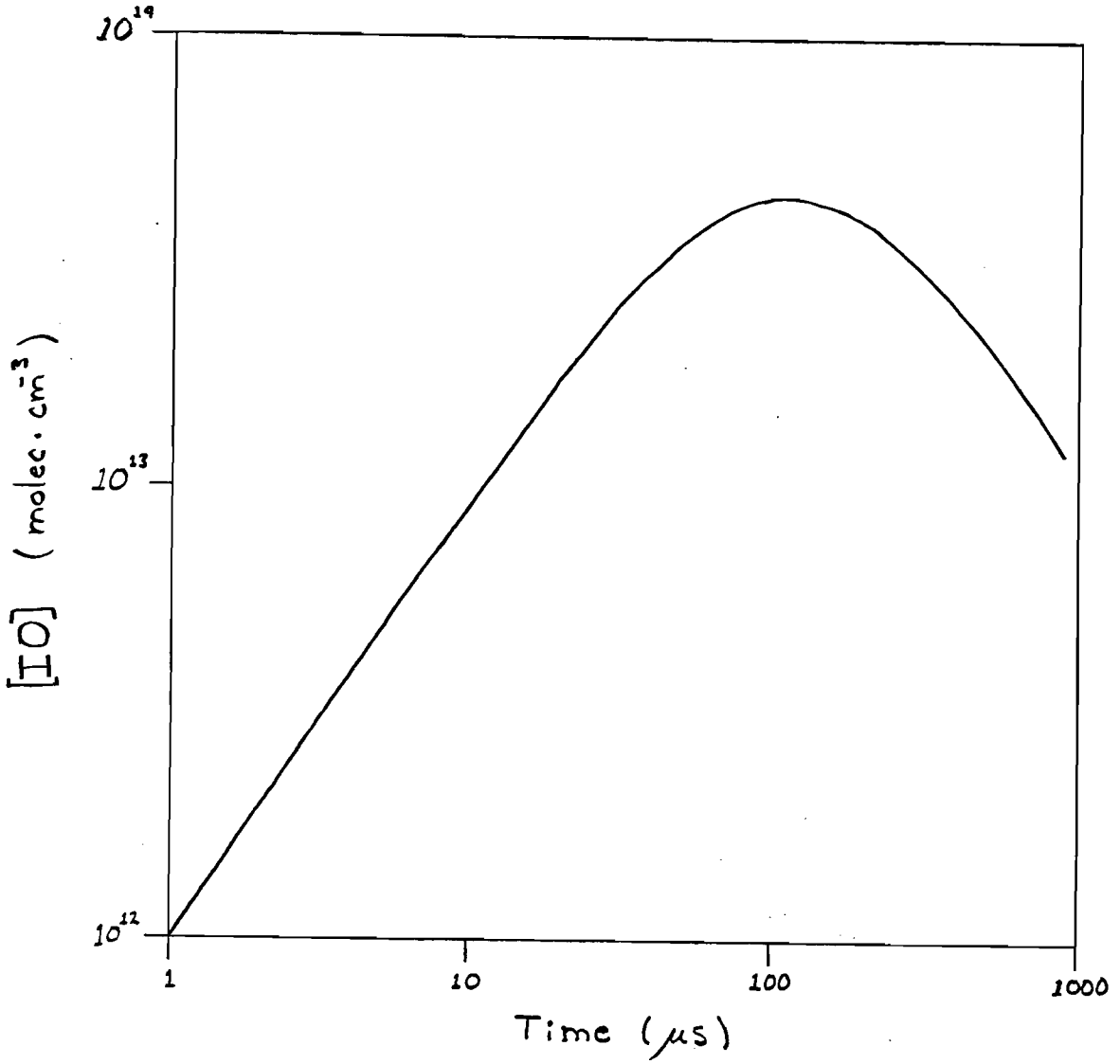

Figure 1: IO concentration in the $I+O_3$ system.

high concentration of IO for the absorption measurement, it is also desirable to keep the I_2 and O_3 densities as low as possible to retard the formation of an opaque deposit on the optical windows, the result of an I_2/O_3 thermal reaction. (The latter reaction has also been noted by Cox and Coker, 1983 and by Jenkin and Cox, 1984). It is thus important to produce as much IO as possible for given I_2 and O_3 levels. For these two reasons the $I + O_3$ production scheme was not used for the bulk of this investigation.

An improved IO production system utilizes the photolysis of ozone at 248 nm as outlined below.

$$O_3 + h\nu(\lambda=248nm) \rightarrow O(^1D) + O_2$$

$$O(^1D) + N_2 \rightarrow O(^3P) + N_2$$

$$4) \quad O(^3P) + I_2 \rightarrow IO + I$$

Here the photolysis and $O(^1D)$ quenching steps may be viewed as occurring instantaneously. The principle competing reactions are,

$$5) \quad O(^3P) + O_3 \rightarrow 2O_2$$

$$6) \quad O(^3P) + O_2 \xrightarrow{M} O_3$$

plus IO lost, as before, via reaction (3).

We note that because I atoms are produced in step (4), rxs 1 and 2 must also be considered. However, as will be seen from our modeling calculations, I atom reactions are sufficiently slow as to be of negligible importance. In a typical experiment the "initial" reactant concentrations are: $[O(^3P)] \simeq 7 \times 10^{13}$, $[I_2] \simeq 5 \times 10^{15}$, $[O_3] \simeq 2 \times 10^{14}$, $[O_2] \simeq 3 \times 10^{16}$ and $[N_2] = 2.5 \times 10^{19}$ (molec$\cdot$cm^{-3}). In this $O + I_2$ system, the initial IO production time constant is $\simeq 2\mu s$. Figure 2 illustrates the resulting IO concentration. The peak IO density under these conditions is nearly 95% of the initial $O(^3P)$ concentration. Thus, the IO level is much less dependent on the rate of reaction (3) and this

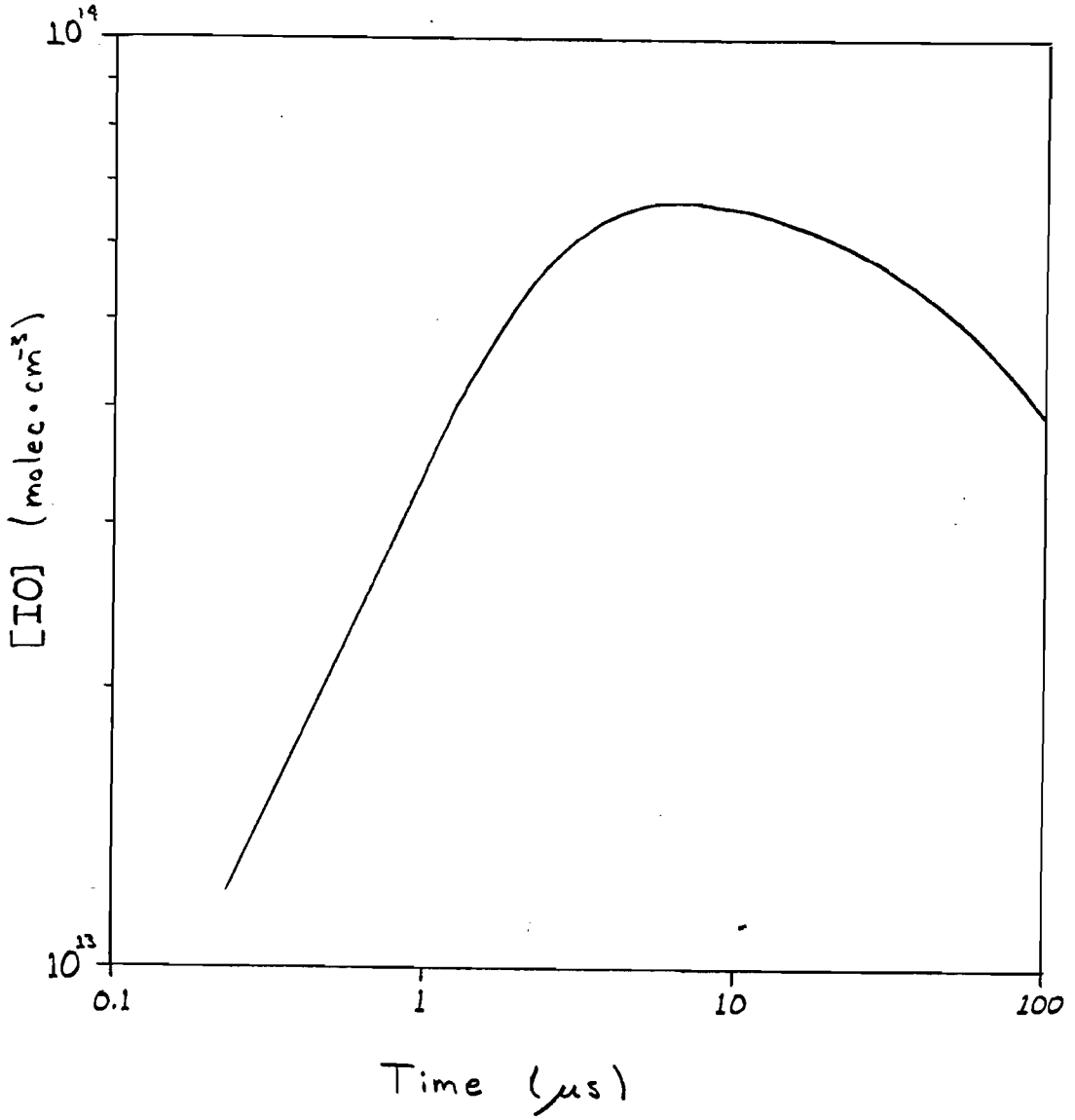

Figure 2 : IO concentration in the $O + I_2$ system.

results in a higher level of IO than that produced in the I + O_3 system for a comparable product of I_2 and O_3 concentrations.

In the HOI absorption measurements the ozone photolysis system was modified in two ways: water was added to the initial mixture and argon was substituted for nitrogen as the carrier gas. The main result of these two changes was to channel the photolytically produced $O(^1D)$ into OH rather than $O(^3P)$, e.g.

7) $O(^1D) + H_2O \rightarrow 2OH$

Some loss of $O(^1D)$ is unavoidable, however, due to the reactions

8) $O(^1D) + Ar \rightarrow O(^3P) + Ar$

9) $O(^1D) + O_2 \rightarrow O(^3P) + O_2$

10) $O(^1D) + O_3 \rightarrow 2O_2$

and 11) $O(^1D) + O_3 \rightarrow 2O(^3P) + O_2$

HOI is formed in the reaction of OH with I_2. Initially this reaction was assumed to be represented by

$OH + I_2 \rightarrow HOI + I$

and measurements of [OH] depletion indicated a rate constant of 1.1 x $10^{-10} cm^3 \cdot molec^{-1} \cdot s^{-1}$. Figure 3 shows the resulting model prediction of the time dependence of [HOI] in a mixture with [OH] ∎ 3 x 10^{14},[H_2O] ∎ 2 x 10^{17},[I_2] → 1 x 10^{15}, [O_3] ∎ 3 x 10^{14}, [O_2] ∎ 5 x 10^{16} and [Ar] ∎ 2.5 x 10^{19}, typical of experimental conditions. In this case the HOI concentration is seen reaching a plateau in under 100μs. Subsequent measurements of the time dependence of [HOI] revealed that this plateau is not reached for 1 to 2 milliseconds after photolysis. This discrepancy suggests that the HOI formation reaction may involve at least two steps. We propose the following mechanism as the simplest one which is consistent with our observations.

12) $OH + I_2 \rightarrow X$

13) $X \rightarrow HOI + I$

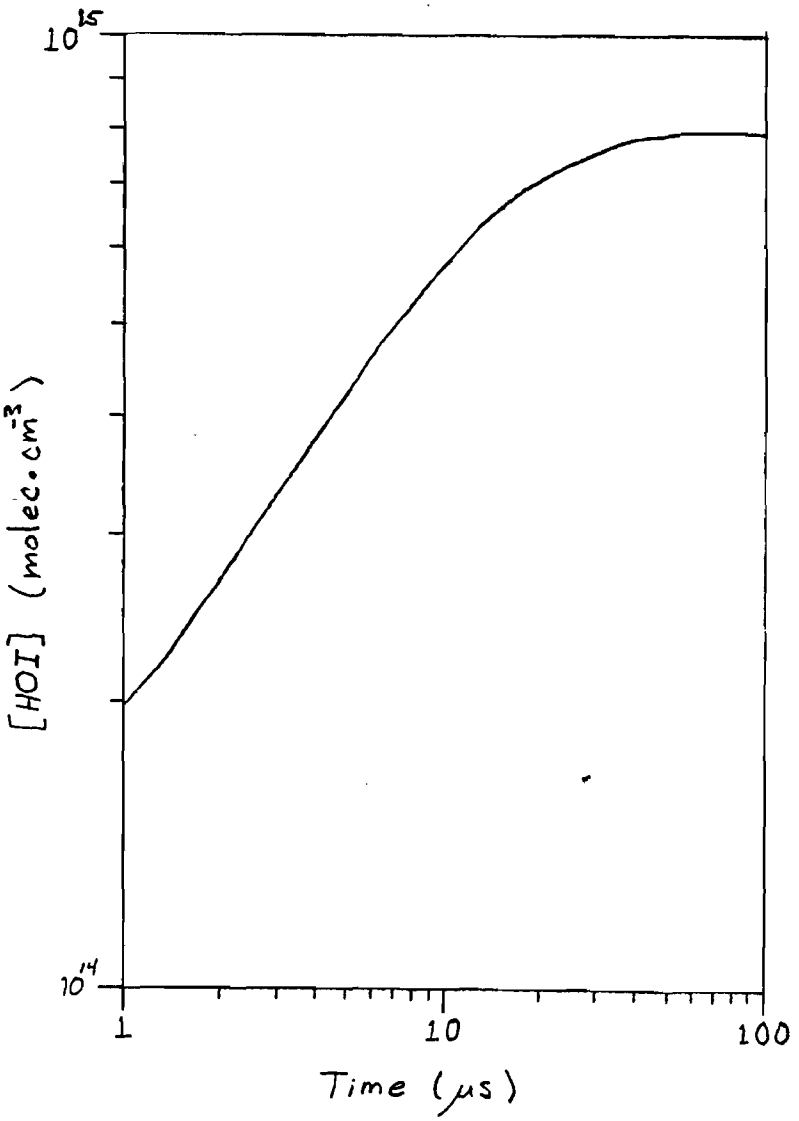

Figure 3: Predicted HOI concentration assuming single-step formation ($OH + I_2 \rightarrow HOI + I$).

Two OH processes which compete with reaction (12) are:

14) $OH + OH \rightarrow H_2O + O(^3P)$

and 15) $OH + OH \xrightarrow{M} H_2O_2$

Alternatively, the hydroxyl radical may be involved in the HOI loss reaction

16) $OH + HOI \rightarrow IO + H_2O$

and in a secondary HOI formation channel

17) $OH + I \xrightarrow{M} HOI$

However, estimates of the rate coefficients for rxs (16) and (17) suggest that both are unimportant compared to rxs (14) and (15).

All of the modeled kinetics curves presented here were generated by a computer code (Fischer, 84) which numerically integrated the complete set of rate equations. This integration is performed in a series of discrete time intervals each involving a two-step linear approximation (Hesstvedt et al., 1978). The concentrations at the beginning of an interval are used to compute derivatives of the form

$$\frac{dC}{dt} = P_o - L_oC$$

for each concentration, C. The production, P_o, and loss, L_o, terms are assumed to be constant for the first half of the interval and the concentrations at the midpoint of the interval, t, are approximated as

$$C_1 = \frac{Po}{L_o} + \left(C_o - \frac{Po}{L_o}\right) \exp\ (-L_ot)$$

These midpoint concentrations are then used to compute a second set of production and loss coefficients, P_1, L_1. Finally, the concentrations at the end of the interval, 2t, are expressed as

$$C_2 = \frac{P_1}{L_1} + \left(C_o - \frac{P_1}{L_1} \right) \exp\ (-L_1\ 2t).$$

The apparatus originally proposed for the IO and HOI absorption measurements included a broadband, pulsed light source and a multi-channel optical array detector. With this system large portions of the spectra under study could have been acquired in a single flash. However, during initial tests of this apparatus, it became apparent that the spectral intensity reaching the optical array was far below initial estimates. The difficulty was traced to a misreprentation by the vendor of the characteristics of the pulsed light source. Subsequent investigations, including attempts to construct a suitable flashlamp in-house, showed that the multi-channel approach was not tractable at that time. It was then decided to conduct the entire spectral investigation using the narrow band technique originally proposed for detailed, high resolution studies of a few isolated lines.

The optical configuration of the final apparatus is shown schematically in figure 4. The photolysis laser was either an ILS NT-674 Nd:YAG, which with a second harmonic generator produced about 40 mJ per shot at 532 nm at the sample cell, or a Quanta Ray model EXC-1 operating with KrF which at 248 nm provided 20 to 40 mJ per shot.

The pulse duration of both lasers was about 10 ns. The YAG beam was expanded by a simple telescope (not shown) and both lasers were apertured to produce a square beam $\approx$ 1.2 cm on a side in the sample volume. The photolysis beam entered and exited the sample cell via uncoated fused silica windows. The beam was usually reversed behind the cell for a second pass. The photolysis energy was periodically measured both before and after the sample cell using a Scientech thermopile.

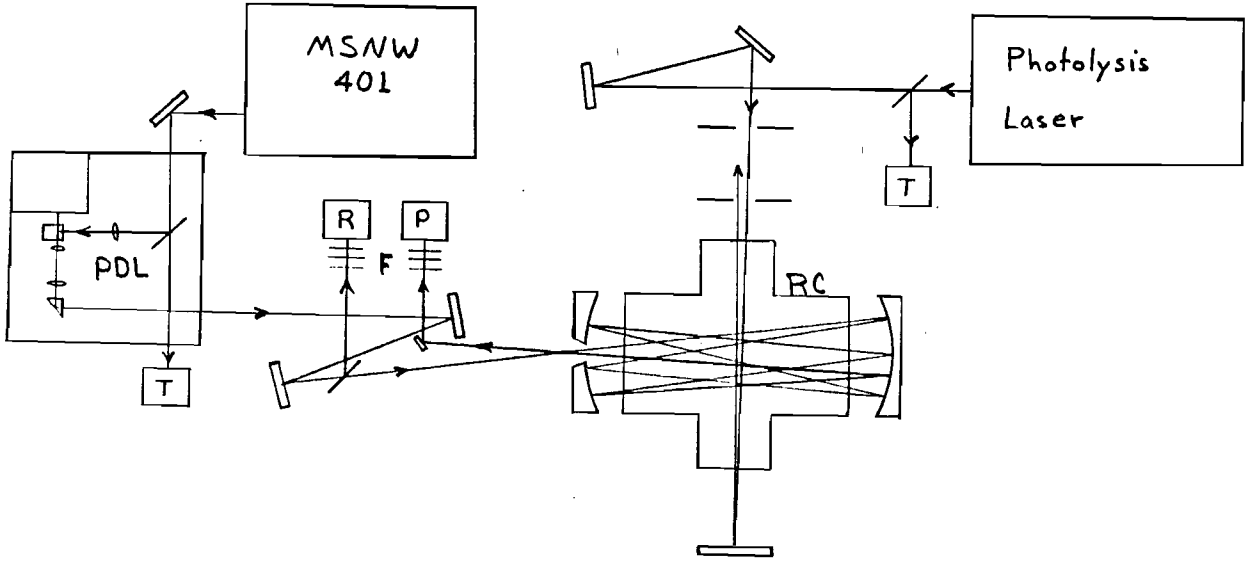

Figure 4: Optical configuration of the IO/HOI apparatus.

P - Probe beam detector

R - Reference beam detector

F - Colored glass filters

RC - Reaction cell

T - Timing diodes

The optical absorption of the photo-produced sample was taken using the output from a Quanta Ray PDL-1 dye laser pumped by a Mathematical Sciences Northwest model 401 excimer laser operating at 308 nm (i.e. XeCl line). The dye laser linewidth was approximately 0.01 nm. The probe beam was passed through the sample 30 to 80 times in a split-mirror, confocal white cell. Optical access was provided by two fused silica windows with multi-layer anti-reflection coatings on both sides. Degradation of these coatings by the sample gases proved to be the primary limitation on the number of passes through the cell. A major source of shot to shot variation in the cell transmission was clipping of the exit beam at the split mirror. This effect was kept to a minimum by pre-focusing the probe beam with the standard PDL telescope. The incident and transmitted probe beam energies were measured by silicon photodiodes, equipped with colored glass bandpass filters, connected to a gated charge integrator. A pair of fast silicon photodiodes allowed an accurate measure of the delay between the photolysis and probe pulses and provided a gating signal for the charge integrator.

Figure 5 is a schematic representation of the gas handling system. With the exception of the pressure regulators on the source gas tanks and the viton o-ring seals used in the reaction cell and optical concentration monitor cells, the entire system contained only pyrex, stainless steel and Teflon. All flows into the reaction cell were metered with thermal capillary mass flow meters. Commercial ultra-high purity gases were used without additional purification as carriers. Total carrier flows from 2 to 15 SLPM were used. Iodine vapor was produced by passing carrier flow gas over reagent grade iodine crystals (Fisher). The concentration of this vapor was monitored by optical absorption at 500 nm. Ultra pure water (Burdick & Jackson) in a high performance bubbler provided a saturated flow of water vapor. Ozone was produced in a silent discharge

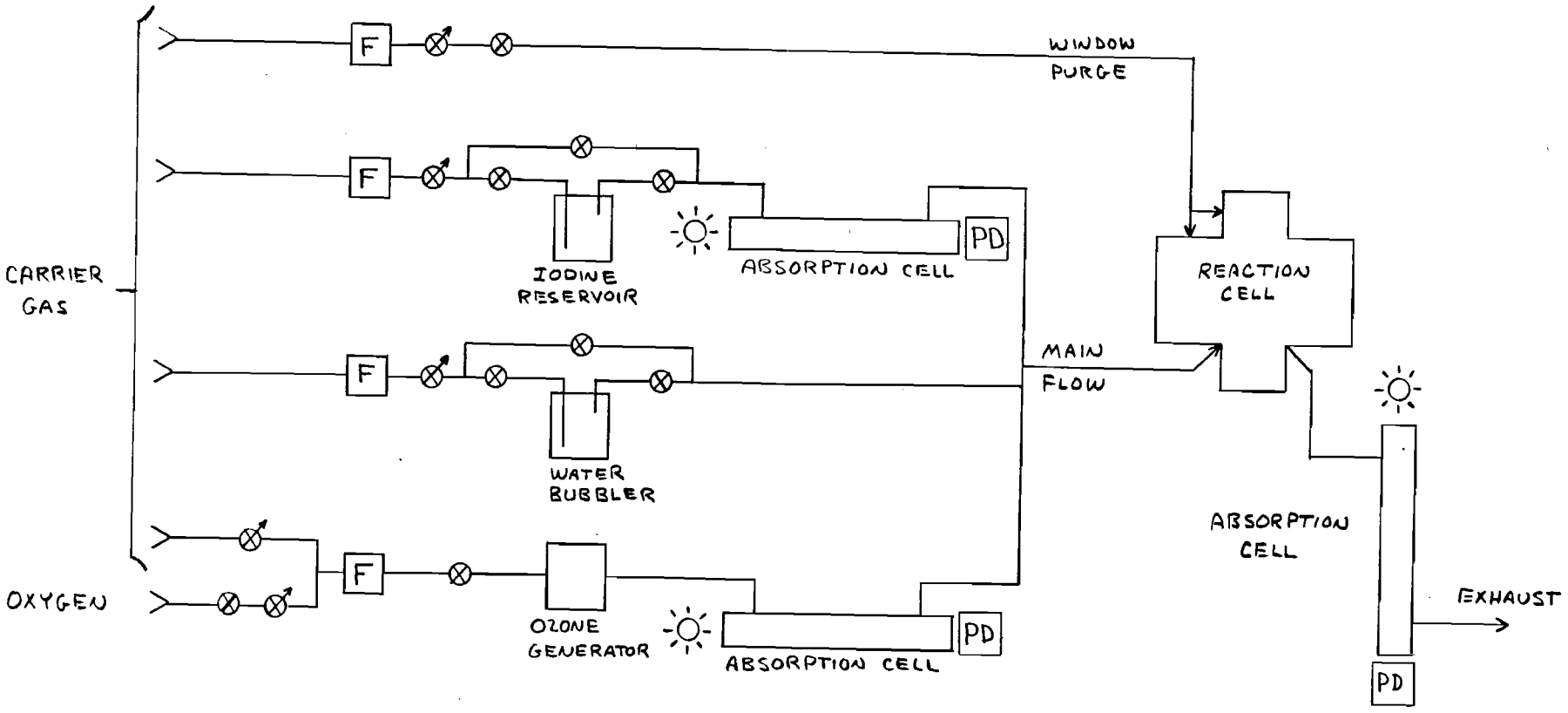

Figure 5: Gas handling system.

F - Capillary flow meter

PD - Photodetector

⊗ - Metering valve

⊗ - Shutoff valve

☼ - Light source

generator (OREC) and monitored by optical absorption at 254 nm. Vapor densities in the reaction cell were calculated from the pre-mixed concentrations and verified by optical absorption downstream. The downstream measurement was reliable for only a short time after beginning an experiment due to the formation of an opaque film on the windows. The optical measurements were based on cross sections of 2.14×10^{-18} cm^2 for iodine (Tellinghuisen, 1973) and 1.11×10^{-17} cm^2 for ozone (Griggs,1968). Cross comparisons and reproducibility checks indicated an overall accuracy of 5 to 10% for the concentration measurements with no window purge flows. Because the purge and sample flows mix at the laser intersection, the extent of the mixing could only be roughly estimated.

A separate apparatus was used in the early stages of this project for a preliminary investigation of the reaction of OH with I_2. OH loss in the presence of excess I_2 was monitored using a laser flash photolysis/laser-induced fluorescence instrument. In this system OH was photolytically produced via the following scheme:

$$O_3 + h\nu \longrightarrow O^1D + O_2$$

$$O^1D + H_2O \longrightarrow 2OH$$

The gas handling system provided a total flow of $\simeq$ 2 SLPM of Ar diluent gas at 1 atm. pressure to the fluorescence/reaction chamber. Ozone was produced by the Hg lamp photolysis of UHP O_2. The concentration of O_2 in the reaction chamber was $\simeq 6.6 \times 10^{17}$ molec$\cdot cm^{-3}$. This system generated a constant O_3 concentration of 2.1×10^{13} molec$\cdot cm^{-3}$ in the reaction cell. Approximately 80% of the Ar diluent was placed through a water bubbler producing 3.3×10^{17} molec$\cdot cm^{-3}$ H_2O in the reaction cell. The addition of I_2 was accomplished by diverting $\simeq$ 18% of the total flow (this being dry Ar) through a trap containing reagent grade I_2 crystal. The 266 nm photolysis laser was $\simeq$ 5 mm in diameter

with a pulse energy of $\pm$ 600 μJ. This beam was crossed with a second 282 nm probe beam ($\pm$ 2.5 nm diameter) which had a pulse energy of $\pm$ 40 μJ. This 282 probe beam was used to excite the Q_{11} ($^2\Pi \rightarrow {}^2\Sigma$) transition in OH. The OH fluorescence was monitored at 310 nm with an interference filter/PMT combination. PMT signal levels were recorded on a gated charge integrator.

III. RESULTS AND DISCUSSION

Spectroscopic and Kinetic Studies Related to the IO Species

The first objective of this study was the measurement of the rate coefficients for reactions (1), (3) and (4). The relative concentration of IO was measured as a function of time after photolysis for several initial conditions. These results were compared to model calculations to determine the rate coefficient values which best reproduced the observed time dependence. The absolute IO concentration calculated from the model was then used to calculate the absolute photoabsorption cross-section at a single wavelength. Finally the entire spectrum was scanned with frequent comparisons to the standard wavelength. A similar procedure was used in the HOI investigation. The details of these results are discussed below.

Table I is a summary of the results from the O + I_2 system. As stated earlier, the initial concentration values are estimated to be accurate to about ± 10%. Statistical errors in the absorbance data are of comparable magnitude so the rate coefficients and cross-sections carry uncertainties of 15-20%. The value obtained here for k_4, $1.44 \pm 0.24 \times 10^{-10}$ $cm^3 \cdot molec^{-1} \cdot s^{-1}$, compares very well with the value of $1.38 \pm 0.44 \times 10^{-10}$ $cm^3 \cdot molec^{-1} \cdot s^{-1}$ reported by Ray and Watson (1981). However, attempts to measure k_4 at elevated levels of I_2 did result in a lower calculated value for k_4. The cause of this discrepancy was found to be in the formation of IO in vibrationally excited states. At high $[I_2]$ the risetime of the IO population in the v=0 level was partially limited by the relaxation time for IO formed with v levels > 0. This effect was discovered by observing absorption in the (3,1) band. The v = 1 population was observed to decay on a time scale of $\simeq$ 10 μs. Figure 6 shows the (3,1) band absorption under the conditions:

$[I_2] = 2.5 \times 10^{15}$ molec·cm^{-3} $\qquad$ $[O] \simeq 4 \times 10^{13}$ molec·cm^{-3}

TABLE I: SUMMARY OF KINETICS RESULTS FROM O + I_2 SYSTEM

$[I_2]$ (10^{14} molec cm^{-3})	$[O_3]$ (10^{14} molec cm^{-3})	$[O]$ (10^{13} molec cm^{-3})	IO+IO k_3 (10^{-11} cm^3 molec$\cdot s^{-1}$)	O + I_2 k_4 (10^{-10} cm^3 $molec^{-1}\cdot s^{-1}$)
2.8	4.3	4.3	6	1.3
3.6	2.9	3.4	6	1.8
5.8	1.7	2.7	6	± 2
6.2	2.7	3.4	6	1.2
9.1	2.0	3.0	5	1.2
9.1	3.3	4.5	8	1.3
11	2.8	2.8	9	1.3

e 6: (3,1) band absorption vs. time.

The influence of IO in v levels > 0 would necessarily be less noticeable at low I_2 concentrations but still should have had a measurable influence on the evaluation of k_4. Thus, the value reported of $1.44 \times 10^{-10} cm^3 molec^{-1} s^{-1}$ may represent a lower limit value. Nevertheless, the error must be reasonably small considering the fact that the value given for k_4 is approaching the gas kinetic collision limit.

In studying reaction (3) (IO + IO), Cox and Coker (1983) measured an effective bimolecular rate coefficient of $4.0^{+2.8}_{-2.0} \times 10^{-10}$ $cm^3 \cdot molec^{-1} \cdot s^{-1}$ at atmospheric pressure. Jenkin and Cox (1984) subsequently studied this rate as a function of pressure from 25 to 400 torr and estimated by extrapolation that the rate coefficient at atmospheric pressure was $1.4 \pm 0.2 \times 10^{-10}$ $cm^3 \cdot molec^{-1} \cdot s^{-1}$. The latter value is ≈ 2.5 times higher than our result of $6.6 \pm 1.1 \times 10^{-11}$ $cm^3 \cdot molec^{-1} \cdot s^{-1}$.

Results from the I + O_3 system were analyzed by taking a value of 6.6×10^{-11} $cm^3 \cdot molec^{-1} \cdot s^{-1}$ for k_3. A value of $1.2 \pm 0.2 \times 10^{-12}$ $cm^3 \cdot molec^{-1} \cdot s^{-1}$ was obtained for k_1 (I + O_3), in good agreement with the value $0.96 \pm 0.3 \times 10^{-12}$ reported by Jenkin and Cox (1984). The absorption cross section of IO at the peak of the (4,0) band was evaluated using our measured values of k_1, k_3 and k_4. The results from both systems, O + I_2 and I + O_3, agree and the composite value is $3.1 \pm 0.6 \times 10^{-17} cm^2$. This value is in good agreement with the $3.1^{+2.0}_{-1.5} \times 10^{-17} cm^2$ value reported by Cox and Coker (1983). The agreement with the more recent result of $2.2 \pm 0.5 \times 10^{-17} cm^2$ from the same laboratory (Jenkin and Cox, 1984) is not as good but is within the stated uncertainties of each study.

All of the spectral measurements in this study were made with a resolution of ≈ 0.01 nm and Figure 7 illustrates a full-resolution spectrograph of the (2,0) bandhead region. The observed linewidths are comparable to the instrumental width. To include all of our data in a reasonable space, we have

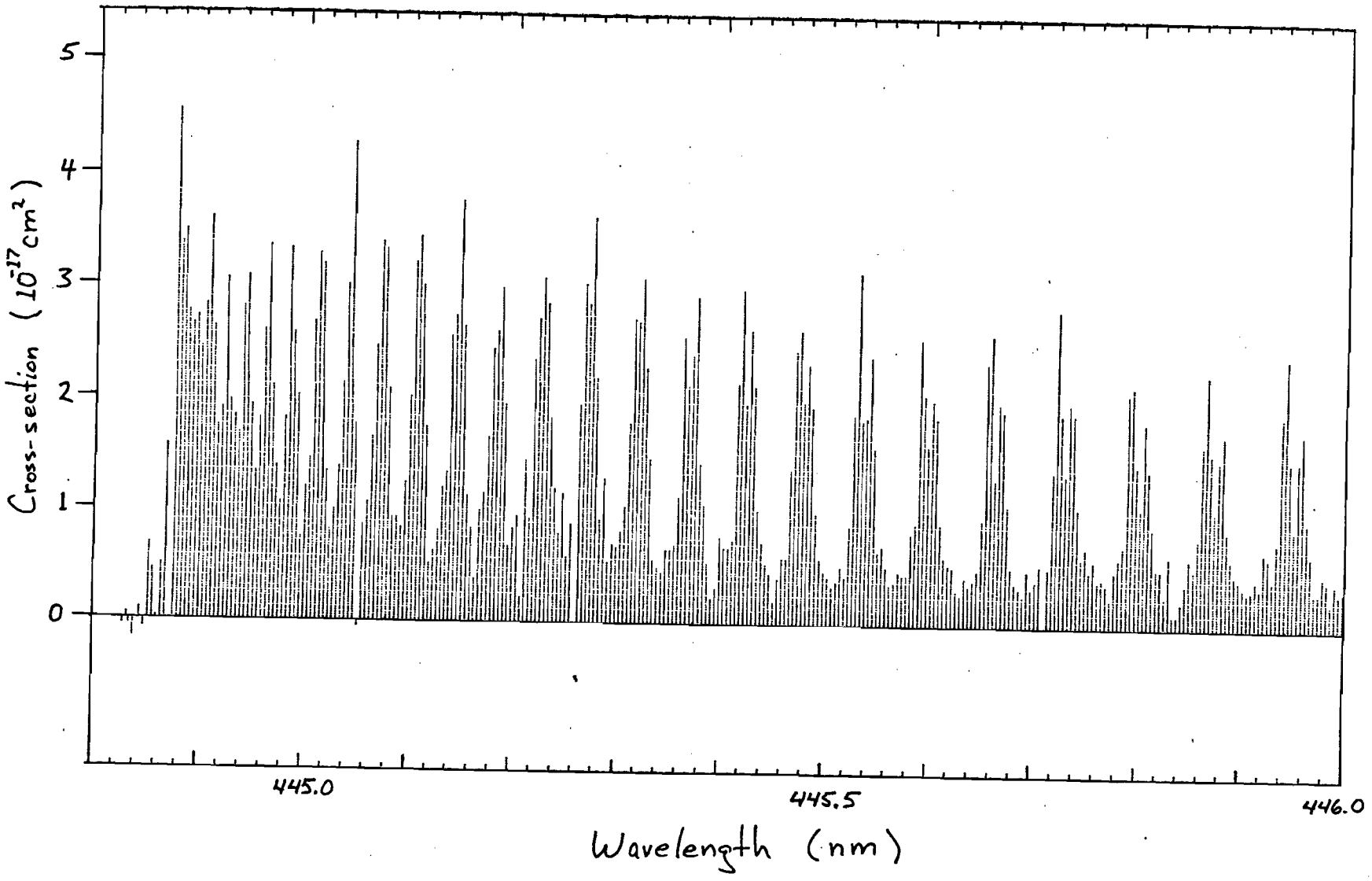

Figure 7: Full resolution spectrum of IO (2,0) band (FWHM ~ 0.01 nm).

smoothed our results to an effective linewidth of ≈ 0.5 nm (FWHM) and included the resulting spectrum as Figure 8. This spectrum is nearly equivalent to that presented by Cox and Coker (1983) (linewidth ≈ 0.27 nm) and should be adequate for the computation of IO photolysis rates in the troposphere. (This exercise is now in progress.)

The observation of the (0,0) band of IO has been a controversial issue for some time. Coleman et al. (1948) first published observations of some 38 IO bands in flow emissions but did not mention the (0,0). Durie and Ramsay (1958) reported seeing the (0,0) band at 465.52 nm in a flame, but later published a more extensive analysis of the IO spectrum (Durie, Legay and Ramsay, 1960) in which nothing at all was said about (0,0). Cox and Coker (1983) reported seeing the (0,0) band in absorption . As evident from figure 8, we were not able to observe any absorption feature in the 466 nm region.

A weak absorption feature has been observed at 410 nm. The spectral position and shape of this band are consistent with the (6,0) band of IO. However, because of the low absorbance, a positive identification of this band was not possible.

Spectroscopic and Kinetic Studies Related to the HOI Species:

The HOI investigation began with a kinetic study involving the measurement of the rate of decay of OH in the presence of I_2, i.e. (12) (OH + I_2). Figure 9 shows the decay of the OH in the presence of I_2. The decay is very nearly exponential with a time constant of ≈ 10 μs. In the absence of I_2 the observed decay time was ≈ 20 ms, indicating the absence of complicating secondary reactions such as (14) or (15).

In the above study the I_2 concentration was estimated to be 50% of saturation or 5.3×10^{15} molec·cm^{-3} at 24°C. This estimate leads to a concentration of 9.5×10^{14} in the reaction cell and hence to a rate coefficient

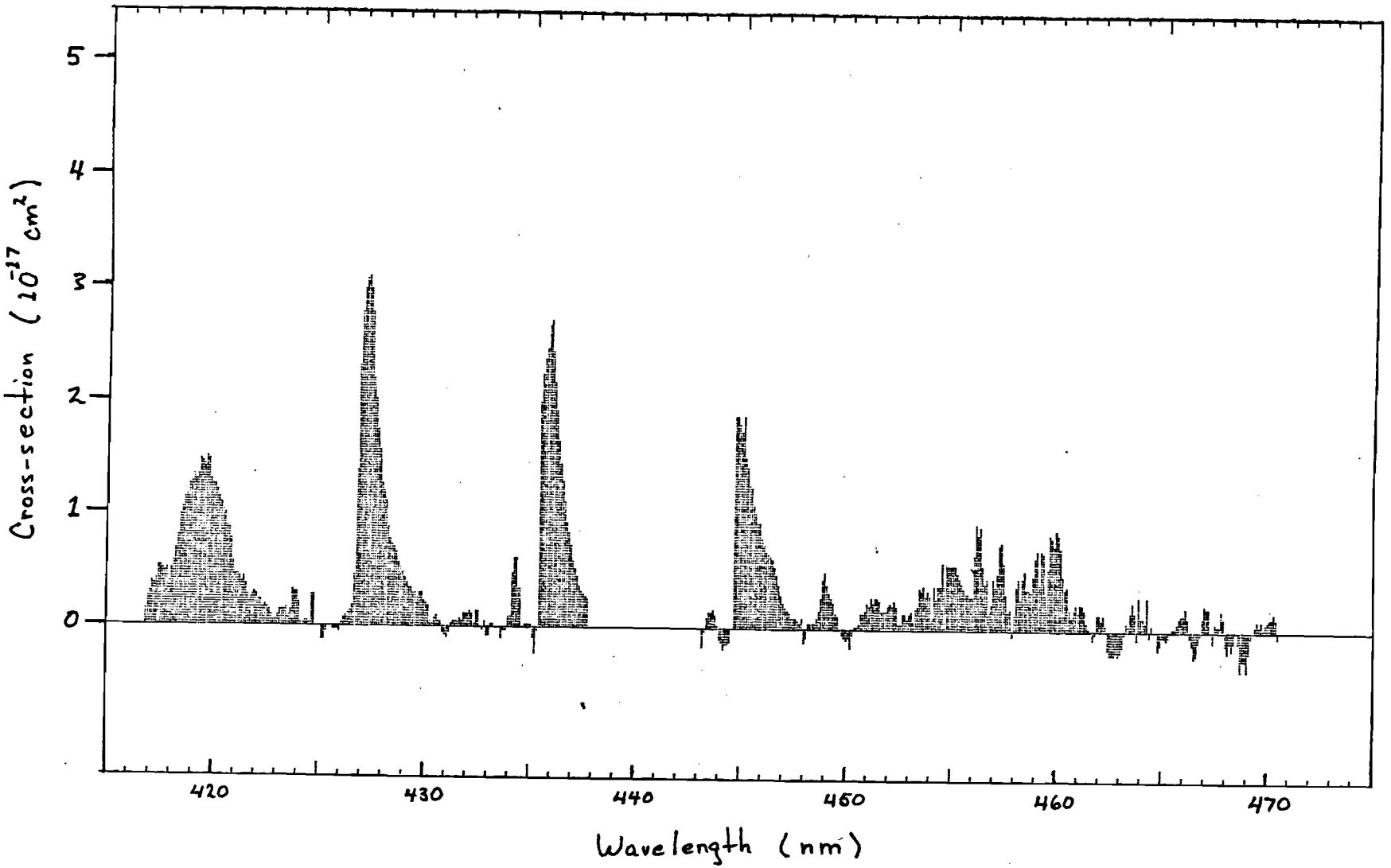

Figure 8: IO absorption spectrum (smoothed to FWHM of 0.5 nm).

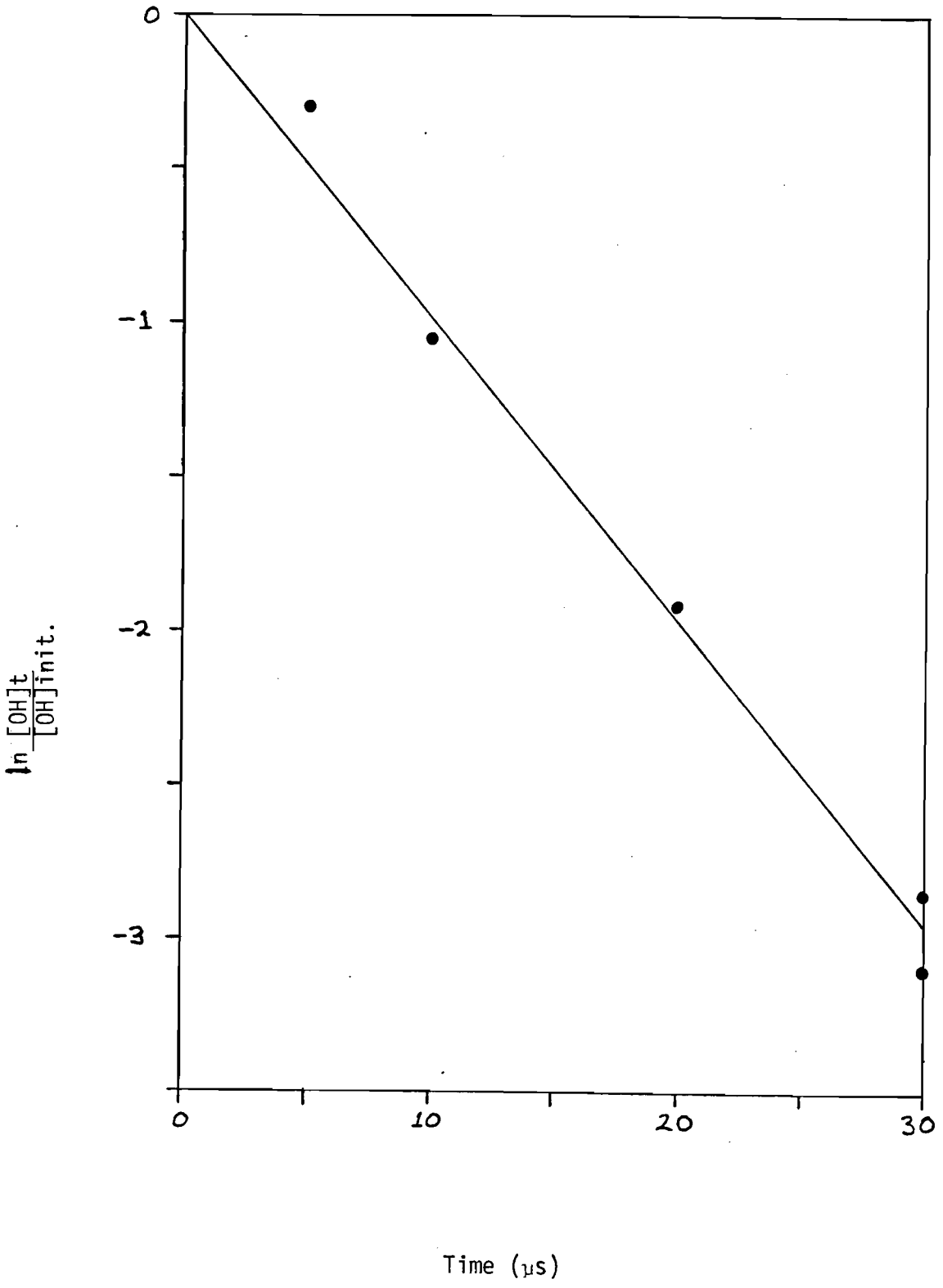

Figure 9: Relative [OH] vs. time after photolysis

of $1.1 \times 10^{-10} cm^3 \cdot molec^{-1} \cdot s^{-1}$ for rx. (12). However, because of the uncertainty in the estimate of $[I_2]$, we believe a conservative value for k_{12} would be:

$$k_{12} = 1.1 \pm 0.6 \times 10^{-10} cm^3 \cdot s^{-1} .$$

Evidence indicating the presence of a reaction complex as proposed earlier

(12) $OH + I_2 \rightarrow x$

(13) $x \rightarrow HOI + I$

is seen in the curve of HOI absorption (at 337 nm) versus time as shown in Figure 10. Although the data are quite scattered, the formation time for HOI is seen to be in the 500 μs range and clearly inconsistent with the OH decay time observed previously. The simplest explanation for this discrepancy is that the absorbing molecule is not HOI. However, the absorption is either highly reduced or totally absent if any of the source constituents, I_2, O_3 or H_2O or the photolysis beam is removed from the reaction mixture. The observed formation time is consistent with our earlier results on reaction (3) ($IO + IO \rightarrow I_2O_2$) but certainly I_2O_2 would form in the absence of water. Furthermore, the similarity between the observed absorption spectrum, shown in Figure 11, and the spectrum of HOCl (JPL,1981) suggests that the absorber is a similar molecule. In view of these facts, we feel that the absorber is probably HOI and that the discrepancy between OH loss and HOI formation rates may be due to a two-step mechanism such as processes (12) and (13).

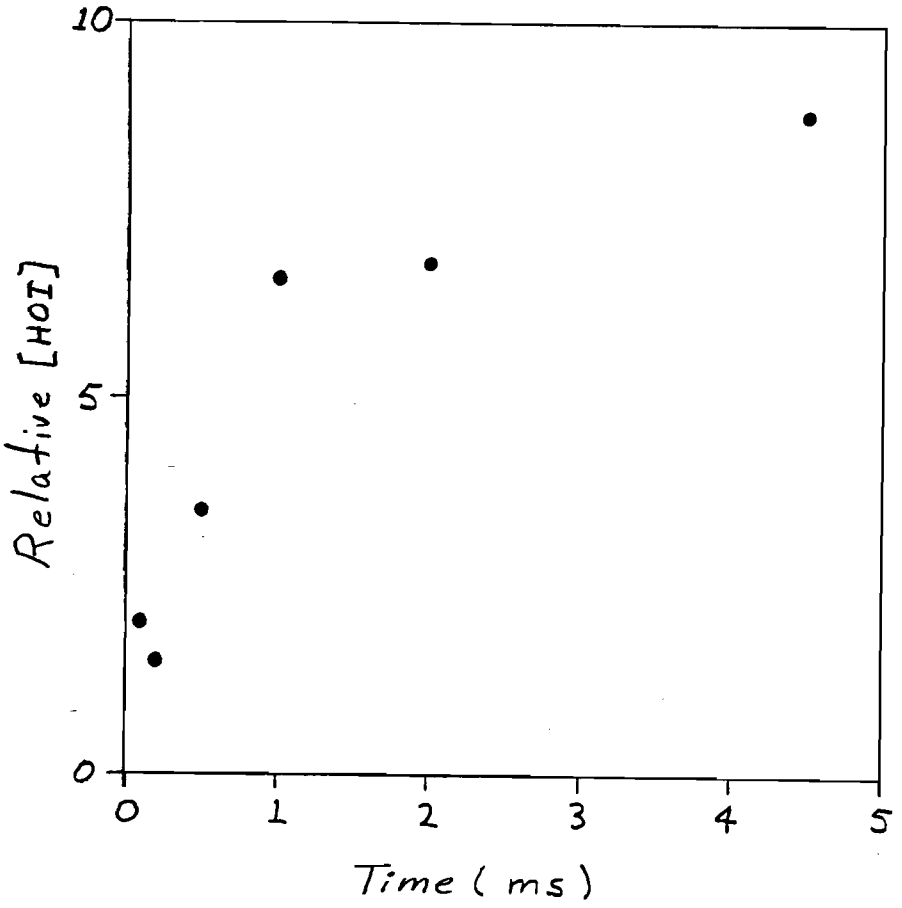

Figure 10: Relative HOI concentration vs. time after photolysis.

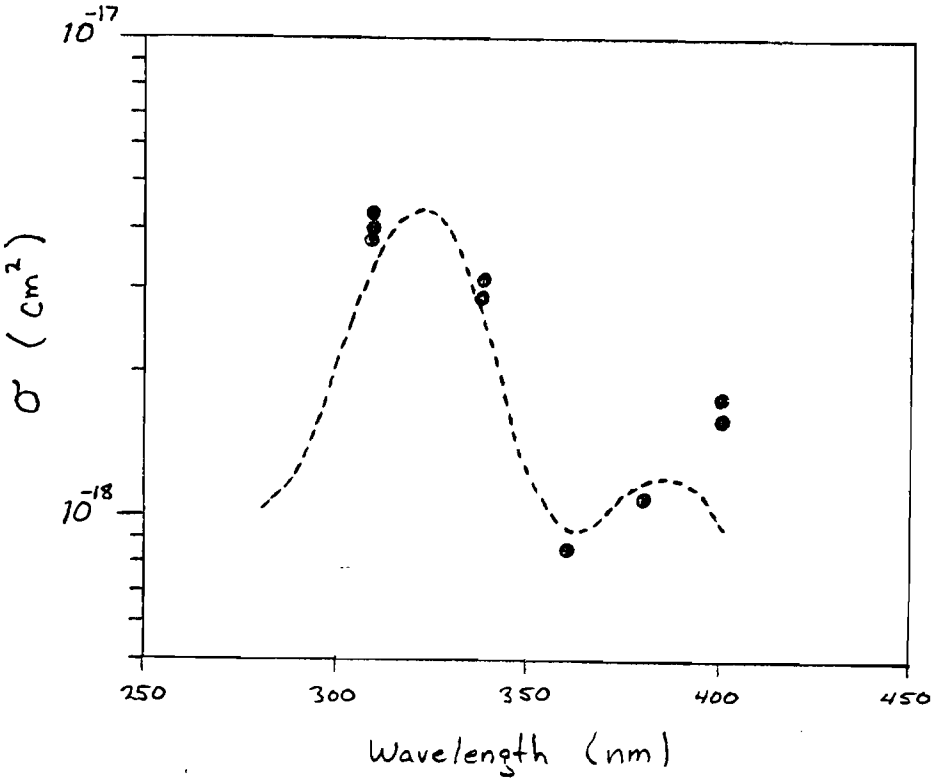

Figure 11: Solid circles are HOI cross-section measurements. Dashed curve represents HOCl spectrum multiplied by 20 and shifted 80 nm toward longer wavelengths.

IV. SUMMARY

A laser flash photolysis apparatus has been used to measure absolute photoabsorption cross sections for the species IO and HOI, as well as rate coefficients for four gas phasereactions involving these molecules. The IO absorption spectrum is consistent with another published result (Cox and Coker, 1983), except in regard to the (0,0) band which was not observed in the present study. The cross section of the (4,0) band was found here to be $3.1 \pm 0.6 \times 10^{-17} cm^2$. The spectrum of HOI was found to resemble that of HOCl, however the peak cross section, $\sigma = 4 \times 10^{-17} cm^2$, is roughly 20 times the HOCl value and peaks at a wavelength of $\approx$ 340 nm. The following rate coefficients were obtained here: $k_1(I+O_3) = 1.2 \pm 0.2 \times 10^{-10}$, $k_3(IO+IO) = 6.6 \pm 1.1 \times 10^{-11}$, $k_4(O+I_2) = 1.44 \pm 0.24 \times 10^{-10}$, $k_{12}(OH+I_2 \rightarrow x) = 1.1 \pm 0.6 \times 10^{-10}$ (all in $cm^3 \cdot molec^{-1} \cdot sec^{-1}$) and $k_{13}(x \rightarrow HOI+I) \approx 2 \times 10^{-3} s^{-1}$. The value for k_3 differs substantially from other measurements (Cox and Coker, 1983; Jenkin and Cox, 1984) while the k_1 and k_4 are in subtantially good agreement with previous investigations. The value of k_{12} and k_{13} are the first to be reported.

Detailed results from this investigation are now being prepared for publication. We anticipate 2 to 3 papers will be forthcoming.

References

Chameides, W. L. and D. D. Davis, J. Geophys. Res., 85, 7383 (1980).

Clyne, M. A. A. and H. W. Cruse, Trans. Farad. Soc., 66, 2277 (1970).

Coleman, E. H., A. G. Gaydon and W. M. Vaidya, Nature, 162, 108 (1948).

Cox, R. A. and G. B. Coker, J. Phys. Chem.,87, 4478 (1983)

Durie, R. A., F. Legay and D. A. Ramsay, Can. J. Phys., 38, 444 (1960).

Durie, R. A. and D. A. Ramsay, Can J. Phys., 36, 35 (1958).

Fischer, S. (Private communication).

Griggs, M., J. Chem. Phys., 49, 857 (1968).

Hesstvedt, E., O. Hov and I. S. A. Isaksen, Int. J. Chem. Kinet., 10, 971 (1978).

Jenkin, M. E., and R. A. Cox (Private communication).

JPL, Publication 81-3, "Chemical Kinetic and Photochemical Data for Use in Stratospheric Modelling - Evaluation Number 4: NASA Panel for Data Evaluation", Jet Propulsion Laboratory, California Institute of Technology, Pasadena, CA. (1981).

Moyers, J. L. and R. A. Duce, J. Geophys. Res. 77, 5229 (1972).

Ray, G. W., and R. T. Watson, J. Phys. Chem., 85, 2955 (1981).

Schofield, K., J. Photochem., 9, 55 (1978).

Tellinghuisen, J., J. Chem. Phys., 58, 2821 (1973).

Zafariou, O. C., J. Geophys. Res., 79, 2730 (1975).

Appendix A

Reactions and rate coefficients used in kinetics models.

With the exception of (13) all rate coefficients are second order, expressed in $cm^3 \cdot molec^{-1} \cdot s^{-1}$. For atomic oxygen, O, represents the ground state, O*, the singlet D state.

1)	$I + O_3 \rightarrow IO + O_2$	$9.6^{(-13)}$	Jenkin and Cox, 1984
2)	$I + I \xrightarrow{M} I_2$	$9.3^{(-13)}$	Chameides and Davis, 1980
3)	$IO + IO \xrightarrow{M} I_2O_2$	$6.6^{(-11)}$	This work.
4)	$O + I_2 \rightarrow IO + I$	$1.38^{(-10)}$	Ray and Watson, 1981
5)	$O + O_3 \rightarrow 2O_2$	$8.9^{(-15)}$	JPL, 1981
6)	$O + O_2 \xrightarrow{M} O_3$	$1.5^{(-14)}$	JPL, 1981
7)	$O^* + H_2O \rightarrow 2OH$	$2.2^{(-10)}$	JPL, 1981
8)	$O^* + Ar \rightarrow O + Ar$	$3^{(-13)}$	Schofield, 1978
9)	$O^* + O_2 \rightarrow O + O_2$	$4^{(-11)}$	JPL, 1981
10)	$O^* + O_3 \rightarrow 2O_2$	$1.2^{(-10)}$	JPL, 1981
11)	$O^* + O_3 \rightarrow 2O + O_2$	$1.2^{(-10)}$	JPL, 1981
12)	$OH + I_2 \rightarrow x$	$1.1^{(-10)}$	This work
13)	$x \rightarrow HOI + I$	$2^{(3)}s^{-1}$	This work
14)	$OH + OH \rightarrow H_2O + O$	$1.8^{(-12)}$	JPL, 1981
15)	$OH + OH \xrightarrow{M} H_2O_2$	$3.65^{(-12)}$	JPL, 1981
16)	$OH + HOI \rightarrow IO + H_2O$	$\leq 8^{(-13)}$	Chameides and Davis, 1980
17)	$OH + I \xrightarrow{M} HOI$	$\leq 5^{(-12)}$	(estimated)